Interannual Variations in Wheat Rust Development in China and the United States in Relation to the El Niño/Southern Oscillation

H. Scherm and X. B. Yang

Department of Plant Pathology, Iowa State University, Ames 50011.
Journal Paper J-16392 of the Iowa Agriculture and Home Economics Experiment Station.
Accepted for publication 2 June 1995.

ABSTRACT

Scherm, H., and Yang, X. B. 1995. Interannual variations in wheat rust development in China and the United States in relation to the El Niño/Southern Oscillation. Phytopathology 85:970-976.

The El Niño/Southern Oscillation (ENSO) is one of the most important and best-characterized mechanisms of global climatic variation. Because regional temperature and precipitation patterns are influenced by the ENSO and plant diseases are responsive to these factors, historical disease records may contain an ENSO-related signal. We used cross-spectral analysis to establish coherence and phase relationships between the Southern Oscillation Index (SOI), which is a measure of the ENSO, and long-term (>40 years) data on wheat stripe rust in five regions of northern China and wheat stem rust in four climatic divisions of the midwestern United States. Monthly SOI values were averaged from March to June and October to March for analysis of the rust data from China and the United States, respectively, based on the times of the year at which weather patterns in these regions are influenced by the ENSO. The coherence relationships showed consistent and significant ($0.01 \leq P \leq 0.10$) cooscillations between the rust and SOI series at temporal scales characteristic of the ENSO. The five stripe rust series were coherent with the SOI series at periodicities of 2.0 to 3.0 and 8.0 to 10.0 years, and three of the four stem rust series were coherent with the SOI series at a periodicity of 6.8 to 8.2 years. The phase relationships showed that, in most cases, the rust and SOI series cooscillated out of phase, suggesting that the associations between them are indirect. In a separate analysis of a shorter (18 years) stripe rust series from the Pacific Northwest of the United States, disease severity was significantly lower during El Niño years (warm phases of the ENSO) than during non-El Niño years ($P \leq 0.0222$) or during La Niña years (cold phases of the ENSO) ($P \leq 0.0253$). Although no cause-and-effect relationships could be deduced, this analysis identified methods and directions for future research into relationships between climate and disease at extended temporal scales.

Additional keywords: Fourier analysis, *Puccinia graminis* f. sp. *tritici*, *P. striiformis* f. sp. *tritici*, scaling, time series analysis.

That plant diseases are strongly influenced by meteorological factors is well established in botanical epidemiology. Numerous studies have linked weather conditions, measured or summarized at various temporal scales, to disease development (7). These studies differ greatly in their scope, ranging from short-term predictions of infection in individual fields with daily or subdaily resolution to medium-term predictions of disease risk over large areas with seasonal or annual resolution. Because of increasing interest in studies of global climatic change (8,26), researchers are now beginning to focus on meteorological variations occurring over periods longer than a few years. However, there is currently little experience with such temporal scales in plant pathology, chiefly because reliable long-term records are lacking for most diseases. Two notable exceptions are wheat stripe rust (*Puccinia striiformis* Westend. f. sp. *tritici*) in northern China and wheat stem rust (*P. graminis* Pers.:Pers. f. sp. *tritici*) in the midwestern United States (western Mississippi Basin), of which long-term (>40 years) records were compiled by Yang and Zeng (33) and Hamilton and Stakman (13), respectively. A shorter (<20 years) record of stripe rust in the Pacific Northwest of the United States was compiled by Coakley et al. (9). These data sets may be useful for studying long-term relationships between climate and disease.

Biologically important effects that are apparent at one temporal scale may not be apparent at other (shorter or longer) temporal scales (18,26,27). The outcome of any study on the effects of meteorological variations, thus, may depend critically on the choice of the scale of attention. Levin (18) and Schneider (27) accentuated the need for a multiscale approach for studying biological patterns or processes over space or time, by which an analysis is carried out simultaneously with respect to multiple units of a measurement. They suggested that spectral and cross-spectral analyses, which are statistical techniques for analyzing periodic patterns in time series over a range of temporal scales (2,22,29), may meet this need.

The El Niño/Southern Oscillation (ENSO) is a global atmospheric fluctuation related to the exchange of air masses between the Eastern and Western hemispheres; it is one of the most important and best-characterized mechanisms of climatic variation and occurs on a temporal scale of 2 to 10 years (4,21). Because regional temperature and precipitation patterns in parts of China (19) and the United States (10,23) are influenced by the ENSO and wheat rusts are responsive to these factors (15), we hypothesized that historical rust records contain an ENSO-related signal. If such a signal along with its characteristic scale could be identified, a basis could be laid for understanding physical relationships between climate and disease at extended temporal scales. This would be important for predicting epidemics several seasons in advance and for assessing the potential impact of global climatic change on disease development.

In this paper, we used cross-spectral analysis to determine at which temporal scales wheat stripe rust in northern China and wheat stem rust in the midwestern United States are associated with the ENSO. We further analyzed the relationship between the

Corresponding author: H Scherm; E-mail address: hwscherm@iastate.edu

ENSO and stripe rust in the Pacific Northwest of the United States; since the latter disease record was too short for cross-spectral analysis, we made pairwise comparisons between disease severity values during El Niño years (warm phases of the ENSO) and non-El Niño years.

MATERIALS AND METHODS

Wheat stripe rust in northern China. Annual data on the severity of stripe rust in five regions of the North-Chinese Plain from 1950 to 1990 (41 years) were documented by Yang and Zeng (33). The regions are Gangu and Xian in the center; and Xinyang, Zhengzou, and Beijing in the southeast, east, and northeast, respectively. Gangu is an important regional source of stripe rust because the pathogen can overwinter and oversummer there. The other regions are dispersal regions: Xinyang is an autumn dispersal region (no oversummering), and Xian, Zhengzou, and Beijing are spring dispersal regions (no overwintering). More detailed accounts of the pandemic system of stripe rust in China have been published previously (33,34). Regional stripe rust-severity values for the five regions were available on a scale from 0 (disease rarely detected) to 4 (destructive yield reductions) in increments of 0.5. Disease severity values in the five regions correlated with each other, with correlation coefficients ranging from 0.56 to 0.84 (33). The data are presented in Figure 1.

Because of the categorical nature of the disease severity values, some regions contained data that departed from a normal distribution. We were unable to alleviate this problem using a general Box-Cox transformation procedure (1). Thus, the significance levels reported for these data sets are only approximations. However, it has been shown previously that lack of normality generally does not negatively influence the results of spectral analyses (22).

Wheat stem rust in the midwestern United States. Annual dates for the first appearance of stem rust in six climatic divisions of the western Mississippi Basin from 1921 to 1962 (42 years) were listed by Hamilton and Stakman (13). We used their data for southeastern Nebraska, east-central South Dakota, southeastern Minnesota, and southeastern North Dakota. The dates of disease appearance in these four divisions correlated with each other, with correlation coefficients ranging from 0.48 to 0.83 (32). Missing data points (between 1 and 3 years per region) were substituted with the appropriate divisional mean of all years. (This procedure had no effect on the variance contained in each record.) Hamilton and Stakman's paper (13) also contained records for north-central Texas and northeastern Kansas, but we did not use these because they had numerous missing values. The data are presented in Figure 2.

Southern Oscillation Index (SOI). Monthly mean values of the SOI were obtained from the National Center for Atmospheric Research, Boulder, CO. The SOI, which is expressed as the double-normalized difference in atmospheric pressure anomalies between Tahiti (in the South Pacific) and Darwin (Australia), is considered a useful measure of the ENSO (5). "Anomaly" refers to the difference between the average pressure for each month and the long-term average of that month; "double-normalized" means that the monthly averages at the two stations, as well as the differences in monthly averages between the two stations, are divided by their long-term standard deviations for that month. SOI values are dimensionless; negative and positive values indicate warm phases and cold phases of the ENSO, respectively (12).

SOI values were summarized differently for northern China and the midwestern United States, based on the times of the year at which weather patterns in these regions are influenced by the ENSO. (These are not necessarily the only times of the year at which wheat rusts are influenced by weather.) For analysis of the

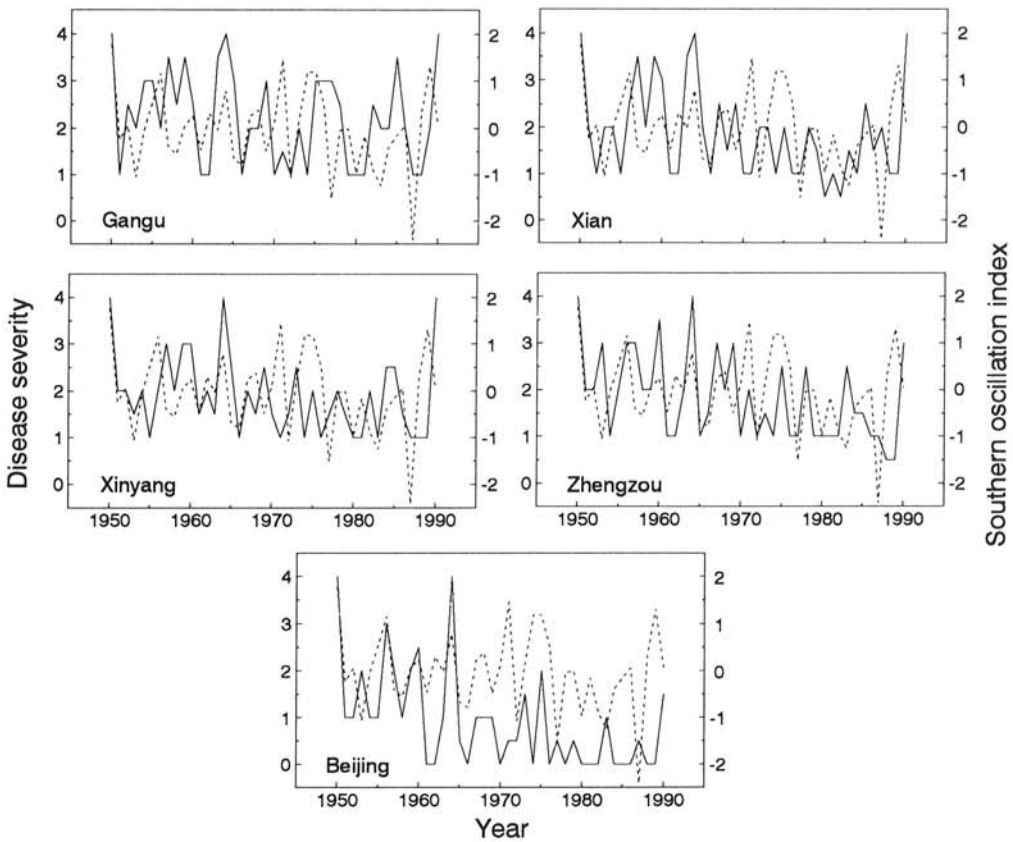

Fig. 1. Time series of annual disease severity values of wheat stripe rust in five regions of northern China in relation to the Southern Oscillation Index (SOI) from 1950 to 1990. Stripe rust severity values (solid lines) are from Yang and Zeng (33) and are given on a scale from 0 (disease rarely detected) to 4 (destructive yield reductions) in increments of 0.5. The SOI (dotted lines) is expressed as the double-normalized difference in atmospheric pressure anomalies between Tahiti (South Pacific) and Darwin (Australia), averaged from March to June.

Chinese stripe rust data, 4-month averages of the SOI were calculated for March to June of each year. The ENSO influences temperature and precipitation during this period in northern China, with spring droughts during warm ENSO phases (19). This period also is critical for epidemic development of *P. striiformis* f. sp. *tritici* (20). The data are presented in Figure 1.

For analysis of the United States stem rust data, 6-month averages of the SOI were calculated for October to March of each year. The ENSO influences temperature and precipitation during this period in the Gulf Coast and Mexican areas (where *P. graminis* f. sp. *tritici* overwinters), with increased precipitation during warm ENSO phases (23). The degree to which the pathogen successfully overwinters during this period is important in determining the first appearance of stem rust in the Mississippi Basin later during spring (3,15,17). The data are presented in Figure 2.

Cross-spectral analysis. We used cross-spectral analysis (2,6, 22,29) to establish relationships between the rust and SOI records over a range of temporal scales. The approach is based on the following principles. Each series (record) is first partitioned into a sum of sine and cosine waves of different amplitudes and harmonics (periodicities) using the finite Fourier transform. This process can be considered a form of analysis of variance in which the total variance of the series is partitioned into contributions of individual harmonics (22). The goal is to identify the harmonics that contribute significantly to the variance of the original series. In an extension of the above procedure, harmonics that contribute significantly to the covariance between two series are identified. The latter procedure provides two useful statistics: the squared coherency, which is a measure of the correlation between two series at each harmonic, and the phase spectrum, which is a measure of the difference in phase between two series at each harmonic. Computational details are given in the appendix.

Before these analyses were carried out, we tested all time series for stationarity (constant means and variances over time) using the unit-root hypothesis test (25). The stem rust series from Nebraska, South Dakota, and Minnesota were nonstationary at $\alpha = 0.05$. Nonstationarity was removed by taking first-order differences of these series (25,29). All series were smoothed using a uniform 5-point moving average before performing cross-spectral analyses (25,29). (Two alternative smoothing windows, a triangular 3-point moving average, and a triangular 5-point moving average also were tested and led to the same conclusions as those given below.) Squared coherency values (K_{xy}^2) and phase spectra between the rust and SOI series were computed using SAS/ETS procedures (2,25). Values of K_{xy}^2 greater than 0.44, 0.53, and 0.68 were considered statistically significant at α-levels of 0.10, 0.05, and 0.01, respectively (14). The null hypothesis was that the rust and SOI series are not coherent (i.e., do not cooscillate) at any temporal scale.

Wheat stripe rust in the Pacific Northwest of the United States during El Niño and La Niña years. Annual disease severity values of stripe rust at Pullman, WA, from 1968 to 1986 were compiled by Coakley et al. (9); data for the susceptible wheat cultivar Omar, used in the present study, were available from 1969 to 1986 (18 years). Disease severity was rated on a scale from 0 (0% disease) to 9 (≥99% disease). Since this time series (Fig. 3) was too short for a multiscale analysis using the methodology described above, we made pairwise comparisons between disease severity values during El Niño years and La Niña years, and between disease severity values during El Niño years and non-El Niño years ("normal" years plus La Niña years) using the median test procedure within SAS/STAT (24). El Niño years (1969, 1972, 1976, 1982, and 1986) and La Niña years (1970, 1973, 1975, and 1978) for the period of interest were designated following Fraedrich and Müller (11).

RESULTS

Wheat stripe rust in northern China in relation to the SOI. The series of annual disease severity values of stripe rust in the five regions of northern China displayed strong interannual fluctuations, without visually apparent synchronization with the SOI series (Fig. 1). However, cross-spectral analysis showed that disease severity values in all regions were significantly coherent with the SOI series at two harmonics (peaks in Fig. 4): the first with a period of 2.8 to 3.0 years (2.0 to 2.1 years for Xinyang), and the second with a period of 8.0 to 10.0 years. For the five regions, half of the squared coherency values at these peaks were significant at $\alpha = 0.01$ ($K_{xy}^2 \geq 0.68$) or $\alpha = 0.05$ ($K_{xy}^2 \geq 0.53$), and the other values at these peaks were significant at $\alpha = 0.10$ ($K_{xy}^2 \geq 0.44$).

The phase spectra showed that there were differences in phase between the rust and SOI series (Table 1). At the 8.0 to 10.0-year peak, the SOI series consistently led the rust series by phase angles

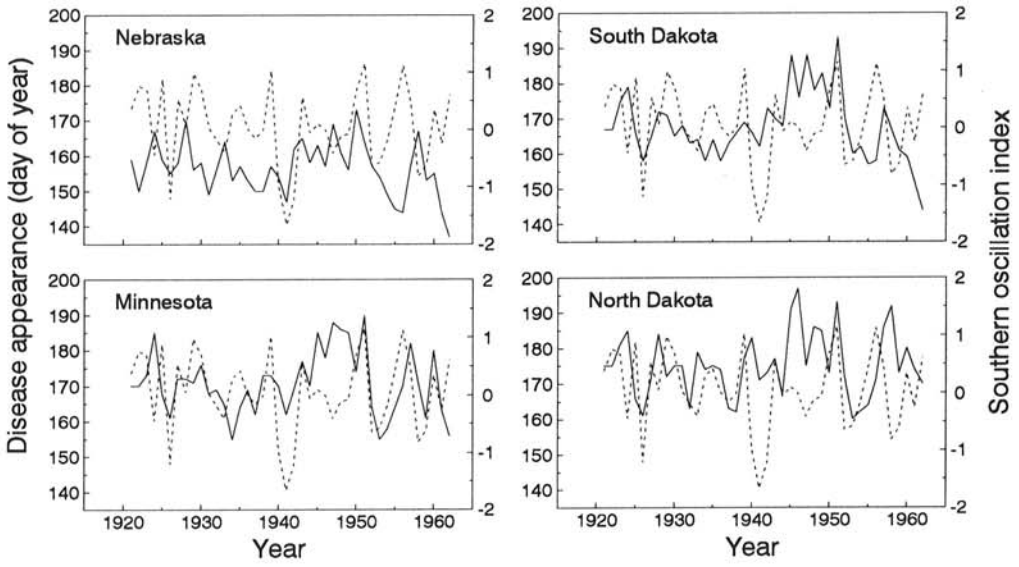

Fig. 2. Time series of annual dates for the first appearance of wheat stem rust in four climatic divisions of the midwestern United States in relation to the Southern Oscillation Index (SOI) from 1921 to 1962. Dates of stem rust appearance (solid lines) are from Hamilton and Stakman (13) and are given as days of the year. The SOI (dotted lines) is expressed as the double-normalized difference in atmospheric pressure anomalies between Tahiti (South Pacific) and Darwin (Australia), averaged from October to March.

of 0.41 to 0.53π radians (1.6 to 2.1 years). At the 2.8 to 3.0-year peak, there were consistent phase relationships between the two series in Xian, Zhengzou, and Beijing (the spring dispersal regions), where the rust series led the SOI series by phase angles of 0.83 to 0.86π radians (1.1 to 1.2 years). The SOI series led the rust series in Gangu (the source region) by a phase angle of 0.35π radians (0.5 years), and the two series were approximately in phase at the 2.0 to 2.1-year peak in Xinyang (the autumn dispersal region).

Wheat stem rust in the midwestern United States in relation to the SOI. Annual dates for the first appearance of stem rust displayed interannual fluctuations, with similar patterns among the four climatic divisions; there was no visually apparent synchronization with the SOI (Fig. 2). However, cross-spectral analysis showed that the rust series in South Dakota, Minnesota, and North Dakota (but not in Nebraska) were significantly coherent with the SOI series at a harmonic of 6.8 to 8.2 years (Fig. 5). (For North Dakota, the value of K_{xy}^2 at this peak was significant only at $\alpha = 0.10$.) No interpretation of the increase in K_{xy}^2 for harmonics with periods greater than 20 years, which was observed for Nebraska, South Dakota, and Minnesota (Fig. 5), was made, because these harmonics had only one complete cycle per record.

The phase spectra for the 6.8 to 8.2-year peak showed that the (differenced) rust series was approximately in phase with the SOI series in South Dakota and Minnesota (Table 1) and that the SOI series led the (nondifferenced) rust series in North Dakota by a phase angle of 0.41π radians (1.4 years). No interpretation of the phase relationships for Nebraska was made there was no significant coherence between the two series.

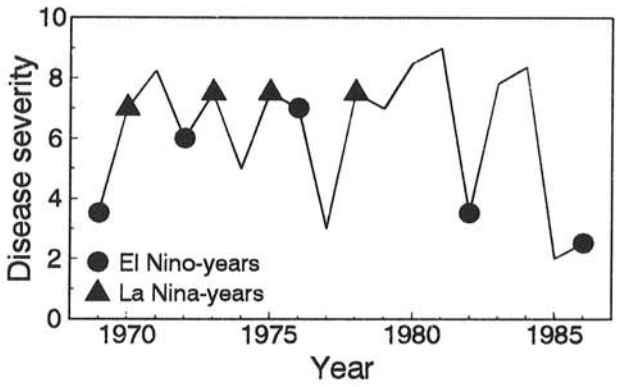

Fig. 3. Time series of annual disease severity values of wheat stripe rust on cultivar Omar at Pullman, WA, from 1969 to 1986. Data are from Coakley et al. (9) and are given on a scale from 0 (0% disease) to 9 (≥99% disease). El Niño and La Niña years were designated according to Fraedrich and Müller (11).

Wheat stripe rust in the Pacific Northwest of the United States during El Niño and La Niña years. The series of annual disease severity values from Pullman, WA, showed strong interannual variations, with lower values during El Niño years than during La Niña years (Fig. 3). (An exception was 1976, an El Niño year in which disease severity reached a value of 7 on a scale from 0 to 9.) According to the median test procedure, disease severity was significantly lower during El Niño years than during La Niña years ($P \leq 0.0253$) or non-El Niño years ("normal" years plus La Niña years) ($P \leq 0.0222$).

DISCUSSION

Associations between within-season variations in weather and epidemics of wheat stripe rust in northern China (20,34) and the Pacific Northwest of the United States (9) and wheat stem rust in the midwestern United States (15,17) have long been established.

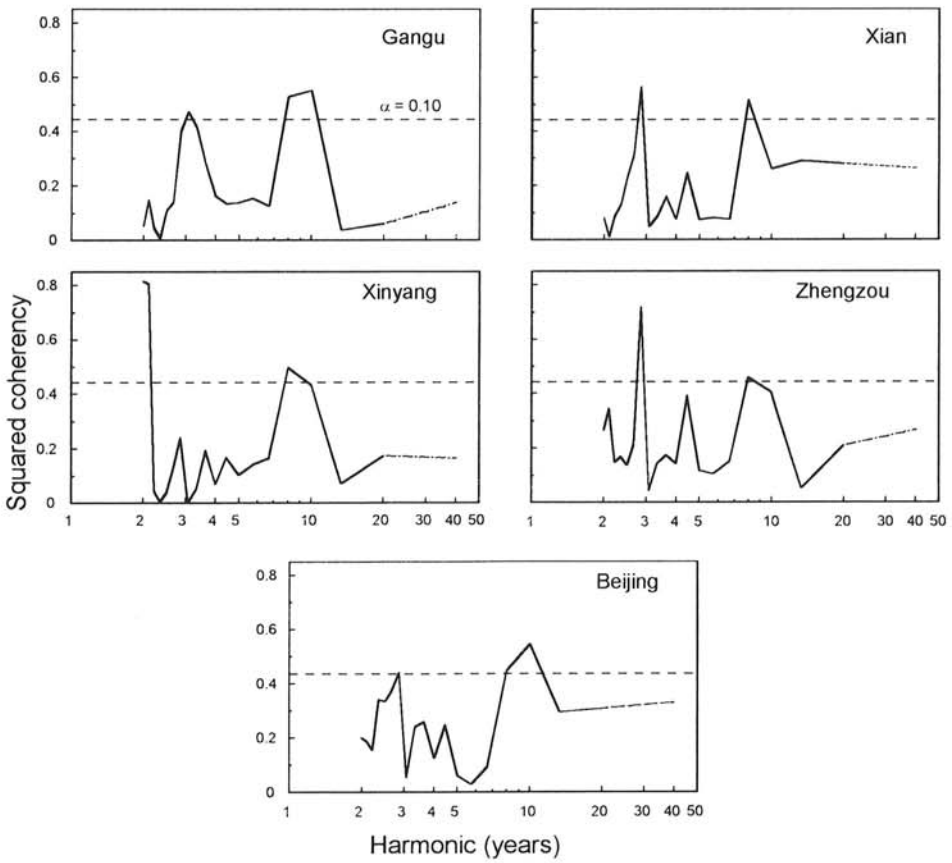

Fig. 4. Coherence relationships among time series of annual disease severity values of wheat stripe rust in five regions of northern China and the Southern Oscillation Index (SOI) from 1950 to 1990. The squared coherency is a measure of the correlation between two series over a range of harmonics (periodicities). The time scale is logarithmic.

However, studies of the relationships between long-term meteorological variations and disease development in these regions are lacking. Such studies could be important for predicting rust epidemics several seasons in advance and for assessing the potential impact of global climatic changes on the two diseases. The present paper attempted to fill this gap by analyzing, over a range of temporal scales, the coherence and phase relationships between regional development of wheat rusts and global meteorological variations of the ENSO.

The coherence relationships showed consistent and significant cooscillations between the rust and SOI series at temporal scales characteristic of the ENSO (2 to 10 years [4,21]). In China, the five stripe rust series were coherent with the SOI series at harmonics of 8.0 to 10.0 and 2.0 to 3.0 years. The former is consistent with a 9.9-year rainfall cycle over China, which has recently been proposed (4) and which may influence rust development during spring. The latter is consistent with the well-established quasi-3-year atmospheric circulation over East Asia, which is known to influence temperature and precipitation in northern China and which is thought to be related to the ENSO (19).

In the United States, three of the four stem rust series were coherent with the SOI series at harmonics of 6.8 to 8.2 years. This is consistent with a quasi-6 to 8-year precipitation cycle over this region (30). It is unknown, however, whether this precipitation cycle is related to the ENSO. In an important climatological study focusing on North America, Ropelewski and Halpert (23) showed that warm ENSO phases commonly are associated with above-average autumn to spring precipitation in the Gulf Coast and Mexican areas (where *P. graminis* f. sp. *tritici* overwinters) but only marginally so in the Mississippi Basin (into which the pathogen is dispersed during spring). Within the latter area, however, associations tended to be stronger in the northern part than in the central and southern parts (Fig. 3 in reference 23). This may explain why, in our study, the rust and SOI series were significantly coherent in North Dakota, Minnesota, and South Dakota but not in Nebraska. However, from a biological viewpoint, it must be borne in mind that precipitation and temperature, even if they were strongly influenced by the ENSO, are not the only factors influencing overwintering of stem rust and its first appearance during spring (15, 17).

The phase relationships were more difficult to interpret than the coherence relationships. For the 8.0 to 10.0-year cooscillation for stripe rust in China, the rust series lagged behind the SOI series by a phase angle of about 0.5π radians (about 2 years). Although this relationship was consistent (it was observed in all five regions), we are not aware of any physical model to explain it adequately. If warm ENSO phases were associated with spring droughts in northern China, as suggested in a recent review (19), one would expect that the rust and SOI series be exactly in phase. In other words, low SOI values (i.e., warm ENSO phases) should correspond to low disease severity values and there should be no phase difference between the series. Since this is not so, the phase re-

TABLE 1. Phase relationships[a] between time series of wheat rusts in China and the United States and the Southern Oscillation Index[b] (SOI)

Disease and region	Phase angle[c] (radians)		
	2.0 to 3.0-yr harmonics	6.8 to 8.2-yr harmonics	8.0 to 10.0-yr harmonics
Wheat stripe rust in China[d]			
Gangu	-0.35π	...[e]	-0.47π
Xian	0.86π	...	-0.41π
Xinyang	0.05π	...	-0.46π
Zhengzou	0.83π	...	-0.53π
Beijing	0.83π	...	-0.46π
Wheat stem rust in the U.S.[f]			
Southeast Nebraska[g]	...	...	...
East-central South Dakota[g]	...	-0.06π	...
Southeast Minnesota[g]	...	0.08π	...
Southeast North Dakota	...	-0.41π	...

[a] Phase relationships are shown only for harmonics with significant coherence relationships.
[b] The SOI is expressed as the double-normalized difference in atmospheric pressure anomalies between Tahiti (South Pacific) and Darwin (Australia). The SOI was averaged from March to June and from October to March for analysis with the stripe and stem rust series, respectively.
[c] Negative phase angle: SOI series is leading; positive phase angle: rust series is leading.
[d] Annual values of disease severity from 1950 to 1990 (33).
[e] Coherence between the rust and SOI series not significant at $\alpha = 0.10$.
[f] Annual dates for the first appearance of stem rust from 1921 to 1962 (13).
[g] Series was differenced before cross-spectral analysis.

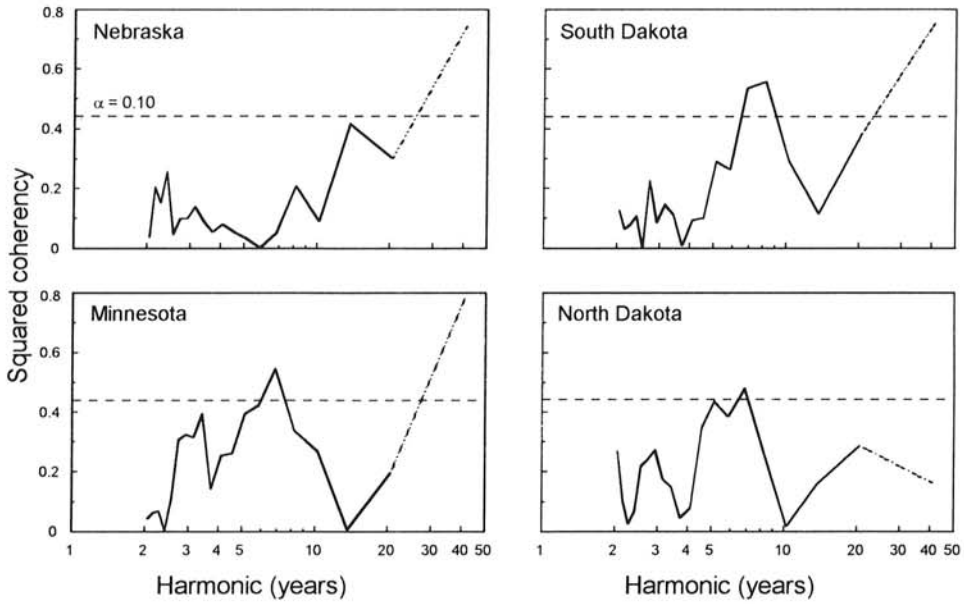

Fig. 5. Coherence relationships among time series of annual dates for the first appearance of wheat stem rust in four climatic divisions of the midwestern United States and the Southern Oscillation Index (SOI) from 1921 to 1962. The squared coherency is a measure of the correlation between two series over a range of harmonics (periodicities). The increase in K_{xy}^2 for harmonics with periods greater than 20 years, which was observed for Nebraska, South Dakota, and Minnesota, cannot be interpreted because these harmonics had only one complete cycle per record. The time scale is logarithmic.

lationships cast doubt on the idea of a direct link between the SOI and stripe rust development in China. A similar conclusion holds for the 2.0 to 3.0-year cooscillation for stripe rust in China and also for the 6.8 to 8.2-year cooscillation for stem rust in the midwestern United States, for which the phase relationships were inconsistent, despite significant coherence relationships.

In the Pacific Northwest of the United States, stripe rust severity was significantly lower during El Niño years than during non-El Niño years. In this region, annual precipitation decreases and the number of days with frost during winter and spring increases during El Niño years (10). Coakley et al. (9) showed that stripe rust development in the Pacific Northwest depends on winter temperature and spring precipitation factors, with limited disease development following low winter temperatures and low spring precipitation. This helps explain the association between the ENSO and rust development in this region when data were analyzed on an annual basis using the median test procedure. However, since this series was too short to perform a multiscale analysis, we were unable to confirm or refute associations between rust severity and the SOI on time scales longer than 1 year.

Further studies of variations in midlatitude meteorological variations (teleconnection patterns) may yield a better physical interpretation for the associations observed in this study. Teleconnections constitute important links between global atmospheric variations (such as the ENSO) and regional weather anomalies (such as excessive precipitation) (12). At least five and seven such patterns have been identified for Northern-Hemisphere winters and summers, respectively (28,31). Teleconnections act by translating global ENSO signals into regional weather events that, in turn, may be related more directly to disease development. In addition to atmospheric links, there also may be oceanic links between the ENSO and regional weather anomalies. For example, planetary-scale oceanic waves generated during the 1982 El Niño are believed to have influenced weather patterns over North Ameria a decade later (16). Similar mechanisms may account for the phase differences between the rust and SOI series observed in our study. This topic remains to be researched further.

A brief discussion of a general limitation of our multiscale analysis seems appropriate. Although spectral and cross-spectral analyses may be used to analyze periodicities with as few as one or two complete cycles per record (4), implying that 16 to 20 years of data would have sufficed to resolve an 8 to 10-year cooscillation, it is undisputed that the reliability of these methods will increase with the length of the data record. A general rule of thumb suggests that 5 to 10 complete cycles should be present to confirm periodic patterns in time series. Thus, the number of observations in our data sets was close to the minimum needed for resolving an 8 to 10-year periodic pattern.

In conclusion, this analysis showed that interannual variations in the development of wheat rusts in China and the United States are associated with the SOI at temporal scales characteristic of the ENSO. However, although the coherence relationships were consistent and significant, the phase relationships indicated that the associations may be indirect and that the causal factor probably lies elsewhere. The ultimate goal of our analysis, to lay a foundation for understanding relationships between climate and disease at extended temporal scales, thus, has not been achieved fully. Although we are unaware of any physical model to explain the observed phase relationships, we suggest that further studies of midlatitude teleconnection patterns may yield a better interpretation for them.

APPENDIX

Spectral analysis assumes that a time series, x_t, with n equally spaced observations ($t = 1,2,3,\ldots,n$), can be modeled as a sum of sine and cosine waves of different amplitudes and harmonics:

$$x_t = \mu_x + \sum_{k=1}^{m} [a_{x,k} \cos(\omega_k t) + b_{x,k} \sin(\omega_k t)] \quad (1)$$

where μ_x is the mean of the time series; $m = n/2$ if n is even or $m = (n - 1)/2$ if n is odd; $k = 1,2,3,\ldots,m$; $\omega_k = 2\pi k/n$ is the frequency of the kth harmonic ($0 \leq \omega_k \leq \pi$); and $a_{x,k}$ and $b_{x,k}$ are the amplitudes of the cosine and sine components of the kth harmonic, respectively.

The periodogram, $I_x(\omega_k)$, which represents the sum of squares for partitioning the total variance of the series into components for each harmonic, is defined as

$$I_x(\omega_k) = \frac{n}{2} (a_{x,k}^2 + b_{x,k}^2) \quad (2)$$

The periodogram is smoothed by a weight function to obtain the smoothed spectral density:

$$\bar{f}_x(\omega_k) = \frac{1}{4\pi} \sum_{j=-d}^{d} W(j) I_x(\omega_{k+j}) \quad (3)$$

where $(2d + 1)$ is the width of the weight function and the individual weights, $W(j)$, sum to unity.

When these procedures are carried out for a second time series, y_t, the cross-periodogram, $I_{xy}(\omega_k)$, which represents the sum of squares for partitioning the covariance of the two series into components for each harmonic, is defined as

$$I_{xy}(\omega_k) = \frac{n}{2} [a_{x,k} a_{y,k} + b_{x,k} b_{y,k} - i(a_{x,k} b_{y,k} - a_{y,k} b_{x,k})] \quad (4)$$

where $i = \sqrt{(-1)}$. The smoothed cross-spectral density is then given by

$$\bar{f}_{xy}(\omega_k) = \frac{1}{4\pi} \sum_{j=-d}^{d} W(j) I_{xy}(\omega_{k+j}) \quad (5)$$

which can be partitioned into a real part, $\bar{C}_{xy}(\omega_k)$, and an imaginary part, $\bar{Q}_{xy}(\omega_k)$:

$$\bar{C}_{xy}(\omega_k) = \frac{n}{8\pi} \sum_{j=-d}^{d} W(j)(a_{x,k+j} a_{y,k+j} + b_{x,k+j} b_{y,k+j}) \quad (6)$$

$$\bar{Q}_{xy}(\omega_k) = \frac{n}{8\pi} \sum_{j=-d}^{d} W(j)(a_{x,k+j} b_{y,k+j} - a_{y,k+j} b_{x,k+j}) \quad (7)$$

The former is the smoothed cospectrum, and the latter is the smoothed quadrature spectrum. The squared coherency, which is a measure of the correlation between the two series at each harmonic, is then defined as

$$K_{xy}^2(\omega_k) = \frac{\bar{C}_{xy}^2(\omega_k) + \bar{Q}_{xy}^2(\omega_k)}{\bar{f}_x(\omega_k) \bar{f}_y(\omega_k)} \quad (8)$$

and the phase spectrum, which is a measure of the difference in phase between the two series at each harmonic, is defined as

$$P_{xy}(\omega_k) = \tan^{-1}\left[-\frac{\bar{Q}_{xy}(\omega_k)}{\bar{C}_{xy}(\omega_k)}\right] \quad (9)$$

The interested reader is referred to Brocklebank and Dickey (2), Platt and Denman (22), or Shumway (29) for further details.

LITERATURE CITED

1. Box, G. E. P., and Cox, D. R. 1964. An analysis of transformations (with discussion). J. Roy. Stat. Soc. 26B:211-252.
2. Brocklebank, J. C., and Dickey, D. A. 1986. SAS System for Forecasting Time Series. SAS Institute, Cary, NC.
3. Burleigh, J. R., Schulze, A. A., and Eversmeyer, M. G. 1969. Some aspects of the summer and winter ecology of wheat rust fungi. Plant Dis. Rep. 53:648-651.
4. Burroughs, W. J. 1992. Weather Cycles: Real or Imaginary? Cambridge

University Press, Cambridge, England.
5. Chen, W. Y. 1982. Assessment of Southern Oscillation sea-level pressure indices. Mon. Weather Rev. 110:800-807.
6. Clendenen, G., Gallucci, V. F., and Gara, R. I. 1978. On the spectral analysis of cyclical tussock moth epidemics and corresponding climatic indices, with a critical discussion of the underlying hypotheses. Pages 279-293 in: Time Series and Ecological Processes. H. H. Shugart, Jr., ed. SIAM Institute for Mathematics and Society, Philadelphia.
7. Coakley, S. M. 1988. Variation in climate and prediction of diseases in plants. Annu. Rev. Phytopathol. 26:163-181.
8. Coakley, S. M. Biospheric change: Will it matter in plant pathology? Can. J. Plant Pathol. In press.
9. Coakley, S. M., Line, R. F., and McDaniel, L. R. 1988. Predicting stripe rust severity on winter wheat using an improved method for analyzing meteorological and rust data. Phytopathology 78:543-550.
10. Cramp, R. P. 1995. El Niño correlates historically with Cascade snowfall. Good Fruit Grower 46(4):6-8.
11. Fraedrich, K., and Müller, K. 1992. Climate anomalies in Europe associated with ENSO extremes. Int. J. Climatol. 12:25-31.
12. Glantz, M. H., Katz, R. W., and Nicholls, N., eds. 1991. Teleconnections Linking Worldwide Climate Anomalies: Scientific Basis and Societal Impact. Cambridge University Press, Cambridge, England.
13. Hamilton, L. M., and Stakman, E. C. 1967. Time of stem rust appearance on wheat in the western Mississippi Basin in relation to the development of epidemics from 1921 to 1962. Phytopathology 57:609-614.
14. Hancock, D. J. 1977. Cross-Spectral Analysis of sunspots and monthly mean temperature and precipitation for the contiguous United States. M.S. thesis. Iowa State University, Ames.
15. Hogg, W. H., Hounam, C. E., Mallik, A. K., and Zadoks, J. C. 1969. Meteorological factors affecting the epidemiology of wheat rusts. World Meteorol. Org. Tech. Note 99:1-143.
16. Jacobs, G. A., Hurlburt, H. E., Kindle, J. C., Metzger, E. J., Mitchell, J. L., Teague, W. J., and Wallcraft, A. J. 1994. Decade-scale trans-Pacific propagation and warming effects of an El Niño anomaly. Nature (Lond.) 370: 360-363.
17. Lambert, E. S. 1929. The relation of weather to the development of stem rust in the Mississippi Valley. Phytopathology 19:1-71.
18. Levin, S. A. 1992. The problem of pattern and scale in ecology. Ecology 73:1943-1967.
19. Liu, Y., and Ding, Y. 1992. Influence of El Niño on weather and climate in China. Acta Meteorol. Sin. 6:117-131.
20. Luo, Y., Shen, Z. R., and Zeng, S. M. 1993. Risk analysis of disease epidemics of wheat by simulation studies. Agric. Syst. 43:67-89.
21. Philander, S. G. H. 1989. El Niño and La Niña. Am. Sci. 77:451-459.
22. Platt, T., and Denman, K. L. 1975. Spectral analysis in ecology. Annu. Rev. Ecol. Syst. 6:189-210.
23. Ropelewski, C. F., and Halpert, M. S. 1986. North American precipitation and temperature patterns associated with the El Niño/Southern Oscillation (ENSO). Mon. Weather Rev. 114:2352-2362.
24. SAS Institute. 1988. SAS/STAT User's Guide. Release 6.03 ed. SAS Institute, Cary, NC.
25. SAS Institute. 1991. SAS/ETS Software: Applications Guide 1. Version 6, 1st ed. SAS Institute, Cary, NC.
26. Scherm, H., and van Bruggen, A. H. C. 1994. Global warming and nonlinear growth: How important are changes in average temperature? Phytopathology 84:1380-1384.
27. Schneider, D. C. 1994. Quantitative Ecology: Spatial and Temporal Scaling. Academic Press, San Diego, CA.
28. Shi, N., and Zhu, Q. 1993. Studies on the northern early summer teleconnection patterns, their interannual variations and relation to drought/flood in China. Adv. Atmos. Sci. 10:155-168.
29. Shumway, R. H. 1988. Applied Statistical Time Series Analysis. Prentice Hall, Englewood Cliffs, NJ.
30. Vines, R. G. 1982. Rainfall patterns in the western United States. J. Geophys. Res. 87:7303-7311.
31. Wallace, J. M., and Gutzler, D. S. 1981. Teleconnections in the geopotential height field during the Northern Hemisphere winter. Mon. Weather Rev. 109:784-812.
32. Yang, X. B. Analysis of the long-term dynamics of stem and leaf rusts of wheat in North America with a time series approach. J. Phytopathol. In press.
33. Yang, X. B., and Zeng, S. M. 1992. Detecting patterns of wheat stripe rust pandemics in time and space. Phytopathology 82:571-576.
34. Zeng, S. M. 1991. PANCRIN, a prototype model of the pandemic cultivar-race interaction of yellow rust on wheat in China. Plant Pathol. 40: 287-295.